Correlation between Persistent Free Radicals of Biochar and Bio-oil Yield at Different Pyrolysis Temperatures

Mei Jiang, Dongmei Bi,* Fupeng Huang, Jiqiang Wang, and Bozheng Li

Biomass pyrolysis technology has important developmental prospects for biofuels and chemicals. Biochar as one of main pyrolysis products has excellent performance in soil improvement and adsorption of harmful elements. The environmentally persistent free radicals (EPFRs) in corn stalk powder and biochar obtained by pyrolysis at different temperatures were tested by electronic paramagnetic resonance spectrometry. After pyrolysis treatment, the biochar had a large number of stable free radicals. With increased pyrolysis temperature, the peak width of the free radicals signal in biochar decreased remarkably, and the widest peak of free radicals signal in biochar was presented at 450 °C, which was 0.69×10^{-4} T. The g-factor of free radicals in biochar decreased continuously as the temperature increased, while the peak height of free radicals first increased and then decreased. The peak height at 600 °C was only 23.8% of the peak height at 500 °C. The concentration of EPFRs in biochar increased with the increase of temperature from 450 °C to 500 °C, while it decreased at higher temperature (>500 °C). This phenomenon was similar to the trend of bio-oil collection efficiency. The experimental results showed a correlation between EPFRs of biochar and bio-oil yield at different pyrolysis temperatures.

Key words: Biochar; Free radicals; Pyrolysis; Electron spin resonance; G factor; Bio-oil

*Contact information: School of Agricultural Engineering and Food Science, Shandong University of Technology, Zibo, Box 255000, China; *Corresponding author: dongmei070719@163.com*

INTRODUCTION

Free radicals are produced by chemical reactions of organic compounds under conditions of light and heat, where homolytic cleavage of covalent bonds forms atoms or groups with unpaired electrons (Forman *et al.* 2015). The electrons in the chemical bond must exist in pairs when the radicals and atoms which contain unpaired electrons form molecules. Accordingly, the free radicals will take electrons from other substances and form a stable substance. This type of reaction is called a free radical reaction (Slater 1984).

Biomass pyrolysis technology is an important way to achieve high-value utilization of biomass. It refers to a process in which the biomass pyrolyzes into pyrolysis oil (tar or bio-oil), biochar, and biogas (mainly containing CH_4, CO, CO_2, and light hydrocarbons), under oxygen-free conditions (Bi *et al.* 2019). Biomass pyrolysis is a complex thermochemical conversion process that includes the fracture and isomerization of molecular bonds, small molecule polymerization, *etc.* The main factors affecting the final product and its distribution of thermal cracking are biomass material properties (type and particle size), pyrolysis reaction temperature, heating rate, gas phase residence time, catalyst, and reaction pressure, *etc.* (Liu *et al.* 2017; Dong *et al.* 2018). There are varieties of biomass pyrolysis processes, but the essence of their chemical reaction is the free radical mechanism (Demirbaş 2000). A weak covalent bond is thermally cleaved to generate fragments containing free radicals, and the process of free radical fragment generation further reacts to form products (Volpe *et al.* 2019). Therefore, in-depth study of the law of free radicals about the process of biomass pyrolysis and the establishment of the relationship between free radicals and reaction products is of great importance for exploring the regulation mechanism of biomass pyrolysis-oriented products.

Electron paramagnetic resonance (EPR) is an important tool for the direct detection and research of paramagnetic materials containing unpaired electrons. Currently, free radical reactions are mainly involved in the fields of fuel combustion, environmental chemistry, polymerization, plasma chemistry, biochemistry, *etc.* They are receiving increased attention (Trubetskaya *et al.* 2016; Valko *et al.* 2016; Lee *et al.* 2019), and it is widely believed that environmentally persistent free radicals (EPFRs) are a new class of environmentally harmful pollutants. Studies have shown that thermal processes, such as biomass burning, coal combustion, and metallurgical industries, can produce EPFRs. These EPFRs can induce the production of free radicals, such as HO·, in the body, causing the biomolecules in the body to be oxidized and then causing DNA damage in the body (Chuang *et al.* 2017).

Gas and persistent free radicals produced by lignite, gas coal, and anthracite are affected by oxidation temperature. The amount of CO and C_2H_4 gas generated during low-temperature oxidation of coal rises gradually as the temperature increases, and the radical concentration also increases with the increase of the oxidation temperature (Petrakis and Grandy 1980). The free radicals in biomass (corn straw, straw, and wheat straw) and biopolymer (cellulose and lignin) biochar can be determined by EPR. The EPR signal has been detected in biochar and remained stable after one month (Liao *et al.* 2014). 9,10-Dihydrophenanthrene(DHP) is a kind of hydrogen donor solvent (typically the partially hydrogenated aromatics) that can provide hydrogen to free radicals produced by pyrolysis. The radicals generated in pyrolysis in the presence of hydrogen donor solvents can be coupled or stabilized by acquiring hydrogen from the solvents, during which the solvents convert to the corresponding aromatics (Curran *et al.* 1967; Kamiya and Nagae 1985). Coal pyrolysis occurs in the presence of dihydrophenanthrene (DHP). The DHP provides hydrogen radicals for the active radicals produced by coal and converts itself to phenanthrene. The change rule of free radicals with the degree of pyrolysis can be quantified by the ratio of phenanthrene to DHP (Liu *et al.* 2016). In this way, the concentration of EPR radicals under hydrogen supply is studied.

Considering that the pyrolysis reaction temperature has an important influence on the composition and distribution of biomass pyrolysis products, this paper studies the influence of different pyrolysis temperatures on the persistent free radicals of straw biochar to explore the reaction mechanism of biomass pyrolysis process for reference.

EXPERIMENTAL

Biomass Sample Processing

The corn stalk used in the experiment was collected from the Zhangdian District, Zibo City, Shandong Province, China. Corn stalk was pulverized with a WF-160 gear-claw disintegrator (Ruifeng Machinery Factory, Jinan, Shandong, China) sieved with a graded vibrating sieve, and then 60-mesh to 100-mesh corn stalk powder was placed in a DHG-9140A electric heating constant temperature blast drying oven (Shanghai Huyueming

Scientific Instrument Co., Ltd., Shanghai, China) and dried continuously at 105 °C for 24 h to constant weight before it was reserved in a sealed bag. Its proximate analysis and elemental analysis data are shown in Table 1.

Table 1. Proximate and Elemental Analysis Results of Biomass (Dry Basis)

Sample	Proximate Analysis (Mass Fraction, %)				Elemental Analysis (Mass Fraction, %)					Higher Calorific Value (kJ/kg)
	Moisture	Ash Content	Volatile Matter	Fixed Carbon	N	C	H	S	O	
Corn Stalks	7.34	6.85	72.69	13.26	1.16	42.86	4.41	0.89	39.16	17725

Experimental Apparatus

The biomass pyrolysis test was completed in an SK2-4-13Q high-temperature horizontal tube furnace (Yahwa Electric Furnace Co., Ltd., Wuhan, Hubei, China) (Fig. 1). The corn stover powder was pyrolyzed under a nitrogen atmosphere, and the pyrolysis temperatures were fixed as 450 °C, 500 °C, 550 °C, and 600 °C, respectively.

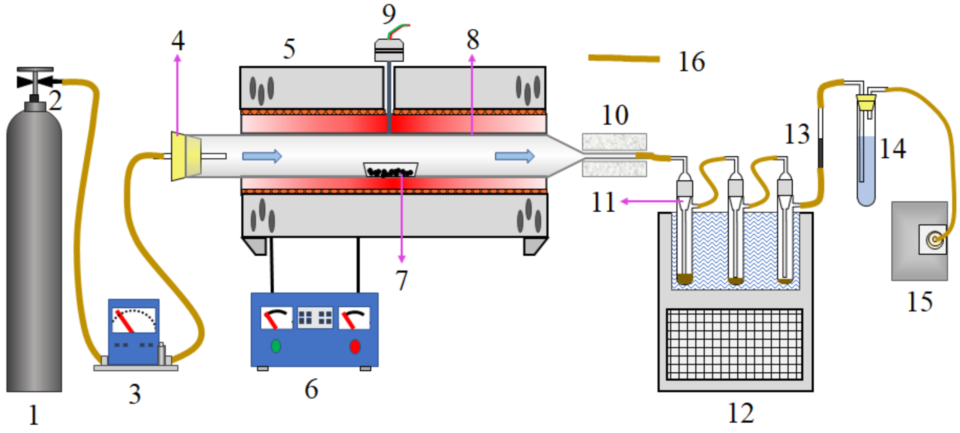

1. N_2 bottle, 2. Valve, 3. Mass flow meter, 4. Rubber plug, 5. Horizontal tube furnace, 6. Control box, 7. Quartz boat, 8. High-temperature resistant quartz tube, 9. Thermocouple, 10. Insulation rock wool, 11. Cold trap, 12. Refrigerated circulator, 13. Gas drying device, 14. Absorption unit of carbon dioxide, 15. Air bag, and 16. Rubber tube

Fig. 1. Schematic diagram of biomass pyrolysis horizontal tube furnace reaction

The target temperature of the horizontal tube furnace was set through the control box. When the horizontal tube furnace reached the set temperature, the nitrogen bottle was opened, with a nitrogen flow rate of 5.00 L/min, and purged for 10 min to drain the air inside the high-temperature resistant quartz tube. Then the nitrogen flow rate was adjusted to 2.40 L/min as the carrier gas flow rate during the pyrolysis of corn stover powder. A sample of 6 g of biomass raw material was evenly spread in the quartz boat, and the quartz boat containing corn stalk powder was quickly placed into the central heating zone of the horizontal tube furnace. The inlet end of the tube furnace was sealed with a rubber stopper to prevent air from entering. After heating for 15 min, the quartz boat was pulled to the vicinity of the inlet end of the horizontal tube furnace, the nitrogen flow rate was adjusted to 5.00 L/min to cool the quartz boat to room temperature. Then, the biochar was removed and weighed before it was placed in an airtight bag that had excluded excess air as an EPR test sample. The outlet end of the high-temperature resistant quartz tube is connected to a three-stage condensing tube, and was placed in a refrigerated circulator set at -10 °C to cool and collect the volatile products generated by pyrolysis. The condensed volatiles in cold traps is bio-oil, and the weight the cold trap increased after pyrolysis is the mass of the bio-oil. The gas products that could not be condensed were purified before discharge.

Measuring Equipment Principle and Test Conditions

There are many compounds that have unpaired electrons in molecular (or atomic) orbits, and there are net electron spins and corresponding magnetic moments, so they have paramagnetic properties (Abragam and Bleaney 2012). The orientation of these unpaired electrons is random in the absence of an applied magnetic field, and they are in the same energy state. When they are subjected to an applied magnetic field, energy level splitting occurs, which is called Zeeman splitting (Yarmus *et al.* 1972). The size of the energy level split is proportional to the strength of the magnetic field. That is, the direction of the electron magnetic moment in the magnetic field is quantized. Different orientation of the magnetic moment and energy result in different magnetic energy levels.

If an electromagnetic wave of frequency v is applied perpendicular to the direction of the magnetic field B, the magnetic field strength and the electromagnetic wave frequency satisfy the following formula (Eq. 1),

$$hv = g\beta B \tag{1}$$

where h is the Planck constant, g is called the g-factor, and β is the nuclear Bohr magneton.

When the frequency of the applied electromagnetic wave is equivalent to the interval of these magnetic energy levels, the electrons in a part of the low energy level absorb the electromagnetic wave energy into the high energy level, which is called electron paramagnetic resonance or electron spin resonance phenomenon (Tonyali *et al.* 2019). Both the concentration and structure information of the free radicals present in the sample can be measured by an electron paramagnetic resonance spectrometer. The system schematic is shown in Fig. 2.

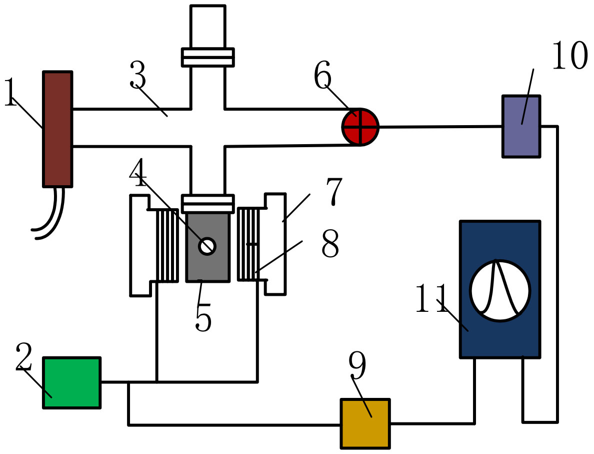

Fig. 2. Principle diagram of free radical measurement in electron paramagnetic resonance device 1. Klystron, 2. Low frequency scanner, 3. Waveguide, 4. Sample, 5. Resonant cavity, 6. Crystal detector, 7. Electromagnet, 8. Scanning coil, 9. Phase shifter, 10. Low frequency amplifier, and 11. Oscilloscope

When biochar was cooled to room temperature, using the MiniScope MS 5000-Bench-Top ESR spectrometer (Magnettech, Berlin, Germany), the free radical test of the obtained biochar completed. The test conditions were a center magnetic field of 337.5 mT, a scan time of 60 s, a microwave power 10 of GHz, a modulation frequency of 100 GHz, a scan width of 5 mT, and a test temperature of 29.4 °C.

RESULTS AND DISCUSSION

Yield of Pyrolysis Three-phase Products of Corn Stalk Powder

The structure of biomass is generally complex, consisting mainly of three major parts of cellulose, hemicellulose, and lignin, as well as a small amount of ash and extract. The exhaust gas produced by corn stalk pyrolysis in the horizontal tube furnace is similar to cigarette smoke, forming a product of aerosol form. At present, almost all collection equipment has low capture efficiency, and it is difficult to obtain complete collection of bio-oil (Park *et al.* 2008). Therefore, the concept of collection efficiency was used to characterize the yield of biomass pyrolysis products, and the formula for calculating the bio-oil collection efficiency S_y (%) is given in Eq. 2,

$$S_y = \frac{Z_y}{Y} \times 100\% \tag{2}$$

where Z_y is the weight (*g*) of the bio-oil obtained in the bio-oil collecting device and Y is the dry weight (*g*) of the biomass material.

The formula for calculating the biochar collection efficiency S_t (%) is given in Eq. 3,

$$S_t = \frac{Z_t}{Y} \times 100\% \tag{3}$$

where Z_t is the weight (*g*) of the biochar obtained in the biochar collecting device.

The formula for calculating the exhaust gas collection efficiency S_q (%) is given in Eq. 4:

$$S_q = 1 - S_y - S_t \tag{4}$$

The collection efficiency of pyrolysis products obtained by corn stalk through the horizontal tube furnace experimental device at different pyrolysis temperatures are shown in Table 2.

Table 2. Effect of Different Pyrolysis Temperatures on Biomass Pyrolysis Products

Pyrolysis Temperature (°C)	Bio-oil Collection Z_y (g)	Bio-oil Collection Efficiency S_y (%)	Biochar Collection Z_t (g)	Biochar Collection Efficiency S_t (%)	Non-Condensable Gas Yield S_q (%)
450	1.82	30.33	2.02	33.67	36.00
500	2.07	34.50	1.73	28.83	36.67
550	1.78	29.67	1.69	28.17	42.16
600	1.80	30.00	1.65	27.50	42.50

Table 2 shows that as the pyrolysis temperature increased, the bio-oil collection efficiency had a maximum at 500 °C, which could reach 34.5%. As the pyrolysis temperature increased, the efficiency of bio-oil collection had a decreasing trend. The biochar collection efficiency had a maximum value of 33.7% at 450 °C. As the pyrolysis temperature increased, the biochar collection efficiency also had a larger value at 550 °C, but the overall trend was a downward trend. With the increase of pyrolysis temperature, the biogas collection efficiency showed a generally increasing trend that reached 42.5% at 600 °C. The test results mentioned above were also consistent with the trend of the existing literature data results.

Analysis of Biochar Persistent Free Radical Test

When the MS5000 was used to measure the free radicals present in the biochar, the free electron absorbing electromagnetic radiation transitioned from a low energy level to a high energy level under an external magnetic field to generate an absorption signal. At this point, the EPR signal spectrum of unpaired electrons could be obtained by detecting the resonant primary differential signal with a high-frequency minor field and a phase-sensitive detector. Figures 3 and 4 show the EPR signal spectra of corn stalk powder and biochar, respectively, where the abscissa indicated the magnetic field strength and the ordinate indicated the resonance absorption intensity.

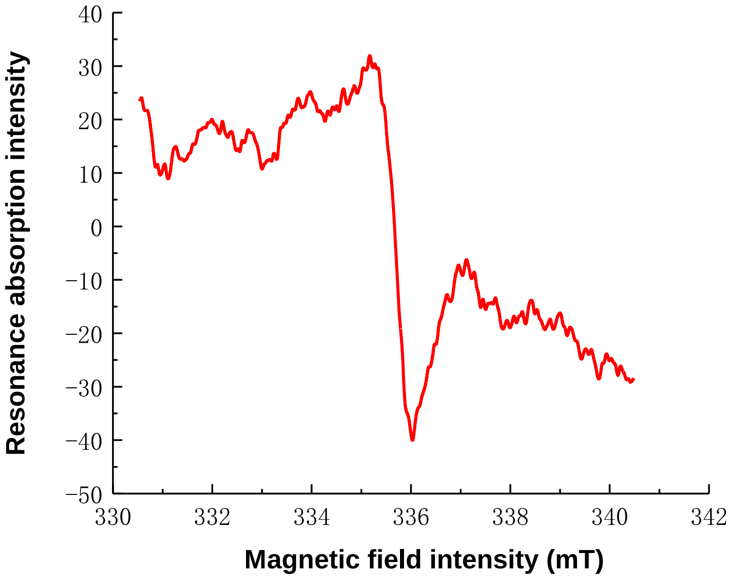

Fig. 3. EPR signal map of corn stalk powder

The EPR spectrum is characterized by a series of parameters such as g-factor, hyperfine structure, fine structure, saturation characteristics, line width, line type, and spin concentration (Adrian *et al.* 1962; Frank *et al.* 1962; Jackson and Wynne-Jones 1964). Among them, line width, g-factor, and spin concentration are the main parameters.

Line width ΔH (also known as peak width), namely the width of the absorption peak, with values in gauss (G), is a parameter that describes the interaction between particles. It is a measure of the interaction of an electron with its surroundings, inversely proportional to the time it takes for the electron to return to the ground state from the excited state of its spin, that is inversely proportional to the relaxation time. The line width is the horizontal distance from crest to trough and can be read directly from the EPR spectrum. The value of the line width is related to the dipole interaction between electrons and their surroundings and the dipole interaction between electrons and nuclei (Mizuochi *et al.* 2009).

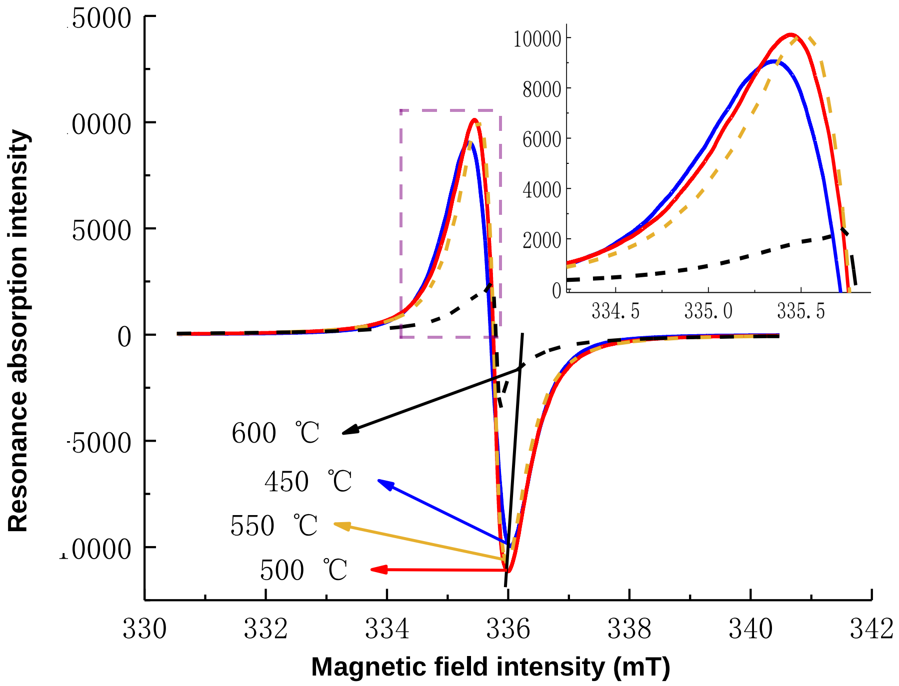

Fig. 4. Free radical signals in biochar obtained by pyrolysis at different temperatures

The *g*-factor (or *g*-value, the Lande factor) determines the position of the line in the EPR spectrum, and it is related to the contribution of spin motion and orbital motion of the electron to the total angular momentum. It depends on the environment of the electron in the molecule and the orientation of the molecule in the magnetic field, and it is a direct factor reflecting the degree of spin orbit interference (Tonyali *et al.* 2019). The *g*-factor is an important parameter for characterizing free radicals. Different free radicals have different *g*-factor values. Accurately determining the *g*-factor can make it possible to judge the influence of electron motion and help to understand the structure of free radicals. For a paramagnetic substance of a specific structure, the *g*-factor is a fixed intrinsic parameter whose size is affected by the spin-orbit coupling effect of the ligand field (or crystal field) environment in which it is located (Modic *et al.* 2014).

The concentration of free radicals (N_g) is also called the concentration of paramagnetic center, that is, the number of free electrons per g of sample. The integral area of the sample paramagnetic resonance line represents the concentration of free radicals in the sample. When the line types of the spectral lines are the same, free radical concentration Ng is proportional to the product of line width ΔH squared and line height H_{pp}, as shown in Eq. 5:

$$N_g \propto \Delta H^2 \times H_{pp} \tag{5}$$

Additionally, the line height and line width are two parameters that determine the area of the EPR spectrum. The radical concentration N_g can be calculated by the following simplified formula shown in Eq. 6,

$$N_g = \frac{H_{pp} \Delta H^2}{G} \times 1.776 \times 10^{17} \tag{6}$$

where H_{pp} and ΔH are the line height and line width, respectively, which are defined in Fig. 5, and G is the signal gain.

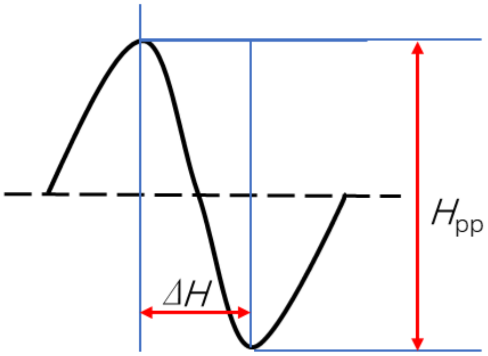

Fig. 5. Definition of H_{pp} and ΔH

Table 3 shows the EPR spectrum parameters of the corn stalk powder and its biochar obtained at different pyrolysis temperatures.

Table 3. EPR Parameters of Corn Stover Powder and Biochar at Different Temperatures

Sample	Peak Height (mm)	Peak Width (10^{-4} T)	Peak Area (Double Credit)	*g*-Value
Corn stalk powder	71.98	0.86	193	2.0050
450 °C biochar	19012.85	0.69	15483	2.0044
500 °C biochar	21257.29	0.55	16905	2.0043
550 °C biochar	20883.09	0.47	15665	2.0041
600 °C biochar	5970.99	0.15	4466	2.0038

The comparison between Figs. 3 and 4, as well as the EPR parameters in Table 3, show that the free radical signal could be detected in the corn stalk powder used in the test, but its EPR signal was weak and almost negligible. This could be obtained from the peak height parameter value of the free radical in the corn stalk powder. This indicated that after the corn stalk was pulverized and dried, a small amount of free radical fragments was produced by itself, which might have been produced in the pulverization process, but the amount of free radicals was small. After pyrolysis treatment, a large amount of free radicals was generated in the obtained biochar, and the free radicals present had potential effects and harmful consequences to the environment.

Table 3 shows that the peak width of free radicals in biochar decreased obviously with the increase of pyrolysis temperature, which was consistent with the trend that the collection rate of biochar decreased with the increase of pyrolysis temperature. The peak width value of biochar obtained by pyrolysis reached the maximum of 0.69 × 10^{-4} T at 450 °C, but it was smaller than the peak width of corn stalk powder. The peak width of biochar at 600 °C was reduced to 0.15 × 10^{-4} T.

Additionally, the *g*-factor of free radicals in corn stalk powder and biochar ranged from 2.0050 to 2.0038 with a slight variation, but all were above the *g*-factor of 2.0023 of free electrons. With the increase of pyrolysis temperature, the *g*-factor of free radicals in biochar decreased continuously. It could be considered that as the pyrolysis temperature increased, the corn stalk powder underwent the reaction of removing heteroatoms during pyrolysis. The reduction of heteroatoms contained in products in biochar resulted in a continuous decrease in the *g*-factor value. Generally, the aromatic or chain hydrocarbon free radical *g*-factor value of the electron in the π orbital is between 2.0025 and 2.0026 (Stone 1963). The single electron is in the oxygen-containing π orbital, such as ether, with a quinone free radical *g*-factor value between 2.0035 and 2.0046 (Hudson and Root 1969). The nitrogen-containing free radical *g*-factor value is 2.0031 (Nakano *et al.* 1990), and the sulfur-containing free radical *g*-factor value is between 2.0050 to 2.0081 (Windle and Wiersema 1964).

As the pyrolysis temperature increased, the peak height of free radicals in biochar first increased and then decreased. The peak height at 500 °C could reach 21257.29 mm, and then the pyrolysis temperature continued to rise. The peak height of free radicals in carbon decreased remarkably, with a peak height of 5070.99 mm at 600 °C, which was only 23.8% of the peak height at 500 °C.

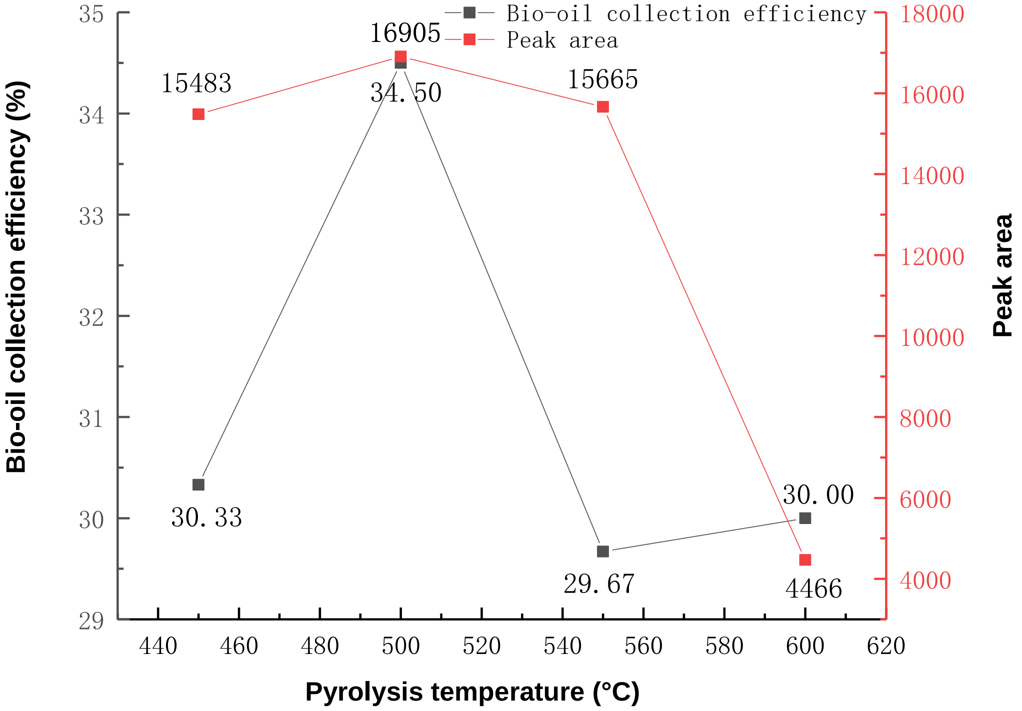

Fig. 7. Bio-oil collection rate and biochar EPR signal peak area at different temperatures

The previous analysis showed that the peak area of EPR spectra could approximately characterize the concentration of free radicals. Figure 7 shows that the concentration of free radicals in biochar increased first and then decreased with the increase of pyrolysis temperature, which was similar to the trend of bio-oil collection efficiency.

Both of them reached the maximum at 500 °C, which indicated that there was a certain internal relationship between them. It could be considered that when the pyrolysis temperature exceeded 450 °C, the covalent bonds in the biomass powder material began to break in a large amount, the O and H elements were continuously removed, the biomass coke was further carbonized, the large compound molecules were rearranged, and the carbon atoms were shared, which formed a large number of free radicals with unpaired electrons during the pyrolysis process, and the paramagnetic signal of the biochar reached the maximum at 500 °C. As the pyrolysis temperature continued to increase, the biochar continued to be charred and decomposed. The highly-active free radicals combined with other molecules to generate a large amount of small molecular gases that volatilized from the biochar to form pyrolysis gas, which caused biochar, the concentration of free radicals, and the rate of bio-oil collection to decrease remarkably.

Volatile free radicals and non-volatile free radicals are produced when heavy organic substances are heated. Non-volatile free radicals on solid surfaces cause structural instability, and then *in situ* condensation forms relatively stable structures, which is not conducive to the further reaction of non-volatile free radical fragments. The higher pyrolysis temperature can break the structure formed by *in situ* polycondensation, allowing for further reaction between the non-volatile radical fragments or reacting with volatile radical fragments to form volatile products. Thus, the concentration of free radicals in the biochar obtained at a pyrolysis temperature of 600 °C was lower than the free radical concentration of the biochar obtained at 550 °C, 500 °C, or even 450 °C.

It could be seen that the concentration of free radicals in biochar was the result of a combination of internal and external factors, and that there was a correlation between the biogas collection rate and the bio-oil collection efficiency.

CONCLUSIONS

1. Free radical signals were detected in the pulverized and dried corn stover powder, but the signal was weak and almost negligible. There were a large number of persistent free radicals in the biochar obtained by pyrolysis, and their potential impacts and hazards to the environment need to be considered.
2. Within the experimental range, the peak width of free radicals in biochar decreased noticeably with the increase of pyrolysis temperature. The peak width of biochar obtained by pyrolysis at 450 °C was the largest, which was 0.69×10^{-4} T.
3. With the increase of pyrolysis temperature, the g-factor of free radicals in biochar decreased. The peak height of free radicals increased first and then decreased. The peak height at 600 °C was only 23.8% of the peak height at 500 °C
4. With the increase of pyrolysis temperature, the concentration of free radicals in biochar first increased and then decreased, which was similar to the trend of bio-oil collection efficiency. Both of them reached the maximum at 500 °C, and there was a certain correlation between them.

ACKNOWLEDGEMENTS

This research was sponsored by the China National Natural Science Fund (Grant No. 51606113 and Grant No. 51406108), the Key Research and Development Program of Shandong Province (Grant No. 2017GGX40108), and the Distinguished Expert of the Taishan Scholars of the Shandong Province.

REFERENCES CITED

Abragam, A., and Bleaney, B. (2012). *Electron Paramagnetic Resonance of Transition Ions*, Oxford University Press, Oxford, United Kingdom.

Adrian, F. J., Cochran, E. L., and Bowers, V. A. (1962). "ESR spectrum and structure of the formyl radical," *J. Chem. Phys.* 36(6), 1661-1672. DOI: 10.1063/1.1732794

Bi, D., Li, B., Liu, S., Yi, W., Jiang, M., and Lin, Z. (2019). "Influence of pyrolysis and torrefaction pretreatment temperature on the pyrolysis product distribution," *BioResource*s 14(1), 1185-1197. DOI: 10.15376/biores.14.1.1185-1197

Chuang, G. C., Xia, H., Mahne, S. E., and Varner, K. J. (2017). "Environmentally persistent free radicals cause apoptosis in HL-1 cardiomyocytes," *Cardiovasc. Toxicol.* 17(2), 140-149. DOI: 10.1007/s12012-016-9367-x

Curran, G. P., Struck, R. T., and Gorin. G. (1967). "Mechanism of the hydrogen-transfer process to coal and coal extract," *Industrial & Engineering Chemistry Process Design and Development* 6(2), 166-173. DOI:10.1021/i260022a003

Demirbaş, A. (2000). "Mechanisms of liquefaction and pyrolysis reactions of biomass," *Energ. Convers. Manage.* 41(6), 633-646. DOI: 10.1016/S0196-8904(99)00130-2

Dong, Q., Niu, M., Bi, D., Liu, W., Gu, X., and Lu, C. (2018). "Microwave-assisted catalytic pyrolysis of moso bamboo for high syngas production," *Bioresource Technol.* 256, 145-151. DOI: 10.1016/j.biortech.2018.02.018

Forman, H. J., Augusto, O., Brigelius-Flohe, R., Dennery, P., Kalyanaraman, B., Ischiropoulos, H., Mann, G., Radi, R., Jackson Roberts, L., Vina, J., *et al.* (2015). "Even free radicals should follow some rules: A guide to free radical research terminology and methodology," *Free Radical Bio. Med.* 78, 233-235. DOI: 10.1016/j.freeradbiomed.2014.10.504

Hudson, A., and Root, K. D. J. (1969). "An electron spin resonance study of some aliphatic and alicyclic ether radicals," *Tetrahedron* 25(21), 5311-5317. DOI: 10.1016/0040-4020(69)80053-0

Jackson, C., and Wynne-Jones, W. F. K. (1964). "Electron spin resonance in carbonized organic polymers—I," *Carbon* 2(3), 227-237. DOI: 10.1016/0008-6223(64)90037-5

Kamiya, Y., and Nagae, S. (1985). "Relative reactivity of hydrogen donor solvent in coal liquefaction," *Fuel* 64(9), 1242–1245. DOI:10.1016/0016-2361(85)90182-6

Lee, Y. H., Lee, K. W., Jeon, G. W., and Lee, C. E. (2019). "Electron paramagnetic resonance and ^{1}H nuclear magnetic resonance study of Y-doping effect on the hydrogen shallow donors in ZnO nanoparticles," *Curr. Appl. Phys.* 19(9), 1015-1018. DOI: 10.1016/j.cap.2019.05.019

Liao, S., Pan, B., Li, H., Zhang, D., and Xing, B. (2014). "Detecting free radicals in biochars and determining their ability to inhibit the germination and growth of corn, wheat and rice seedlings," *Environ. Sci. Technol.* 48(15), 8581-8587. DOI: 10.1021/es404250a

Liu, M., Yang, J., Yang, Y., Liu, Z., Shi, L., He, W., and Liu, Q. (2016). "The radical and bond cleavage behaviors of 14 coals during pyrolysis with 9,10-dihydrophenanthrene," *Fuel* 182, 480-486. DOI: 10.1016/j.fuel.2016.06.006

Liu, Z., Wang, L., Zhang, Y., Li, Y., Li, Z., and Cai, H. (2017). "Cellulose-lignin and xylan-lignin interactions on the formation of lignin-derived phenols in pyrolysis oil," *BioResources* 12(3), 4958-4971. DOI: 10.15376/biores.12.3.4958-4971

Mizuochi, N., Neumann, P., Rempp, F., Beck, J., Jacques, V., Siyushev, P., Nakamura, K., Twitchen, D. J., Watanabe, H., Yamasaki, S., *et al.* (2009). "Coherence of single spins coupled to a nuclear spin bath of varying density," *Phys. Rev. B* 80(4), Article ID 041201. DOI: 10.1103/PhysRevB.80.041201

Modic, K. A., Smidt, T. E., Kimchi, I., Breznay, N. P., Biffin. A., Choi, S., Johnson, R. D., Coldea, R., Watkins-Curry, P., McCandless, G. T., *et al.* (2014). "Realization of a three-dimensional spin–anisotropic harmonic honeycomb iridate," *Nat. Commun.* 5, Article Number 4203. DOI: 10.1038/ncomms5203

Nakano, T., Koike, S., and Ohki, Y. (1990). "Electrical properties of nitrogen-containing plasma polymer films," *J. Phys. D- Appl. Phys.* 23(6), 711-718. DOI: 10.1088/0022-3727/23/6/013

Park, H. J., Dong, J.-I., Jeon, J.-K., Park, Y.-K., Yoo, K.-S., Kim, S.-S., Kim, J., and Kim, S. (2008). "Effects of the operating parameters on the production of bio-oil in the fast pyrolysis of Japanese larch," *Chem. Eng. J.* 143(1-3), 124-132. DOI: 10.1016/j.cej.2007.12.031

Petrakis, L., and Grandy, D. W. (1980). "Free radicals in coals and coal conversion. 2. Effect of liquefaction processing conditions on the formation and quenching of coal free radicals," *Fuel* 59(4), 227-232. DOI: 10.1016/0016-2361(80)90139-8

Slater, T. F. (1984). "Free-radical mechanisms in tissue injury," *Biochem. J.* 222(1), 1-15. DOI: 10.1042/bj2220001

Stone, A. J. (1963). "*g* factors of aromatic free radicals," *Mol. Phys.* 6(5), 509-515. DOI: 10.1080/00268976300100571

Tonyali, B., McDaniel, A., Trinetta, V., and Yucel, U. (2019). "Evaluation of heating effects on the morphology and membrane structure of *Escherichia coli* using electron paramagnetic resonance spectroscopy," *Biophys. Chem.* 252, Article ID 106191. DOI: 10.1016/j.bpc.2019.106191

Trubetskaya, A., Jensen, P. A., Jensen, A. D., Glarborg, P., Larsen, F. H., and Andersen, M. L. (2016). "Characterization of free radicals by electron spin resonance spectroscopy in biochars from pyrolysis at high heating rates and at high temperatures," *Biomass Bioenerg.* 94, 117-129. DOI: 10.1016/j.biombioe.2016.08.020

Valko, M., Jomova, K., Rhodes, C. J., Kuča, K., and Musílek, K. (2016). "Redox- and non-redox-metal-induced formation of free radicals and their role in human disease," *Arch. Toxicol.* 90(1), 1-37. DOI: 10.1007/s00204-015-1579-5

Volpe, R., Menendez, J. M. B., Reina, T. R., Volpe, M., Messineo, A., Millan, M., and Titirici, M.-M. (2019). "Free radicals formation on thermally decomposed biomass," *Fuel* 255, Article ID 115802. DOI: 10.1016/j.fuel.2019.115802

Windle, J. J., and Wiersema, A. K. (1964). "Electron paramagnetic resonance of some sulfur and selenium compounds," *J. Chem. Phys.* 41(7), 1996-2002. DOI: 10.1063/1.1726194

Yarmus, L., Rosenthal, J., and Chopp, M. (1972). "EPR of triplet excitions in tetracene crystals: Spin polarization and the role of singlet exciton fission," *Chem. Phys. Lett.* 16(3), 477-481. DOI: 10.1016/0009-2614(72)80404-4

Article submitted: September 6, 2019; Peer review completed: December 7, 2019;
Revised version received: December 27, 2019; Published: January 8, 2020.
DOI: 10.15376/biores.15.1.1384-1396